



Sixth framework programme of the
European Commission

GOCE-CT-2003-505401

RIVERTWIN

A regional model for integrated water management in twinned river basins

Instrument: Specific Targeted Research Project (STREP)

Priority: Sustainable development, Global Change and Ecosystems

D21 Highly resolved climate scenarios from stochastic model Until 2030 for the Ouémé river basin

Due date of deliverable: Feb 06

Actual submission date: July 06

Start date of project: 01.03.2004

Duration: 3 years

Institute of Hydraulic Engineering, University of Stuttgart

Revision: Final

Project co-funded by the European Commission within the Sixth Framework programme (2002-2006)		
Dissemination level		
PU	Public	X
PP	Restricted to other programme participants (including Commission Services)	
RE	Restricted to group specified by the consortium (including Commission Services)	
CO	Confidential, only for members of the consortium (including Commission Services)	

CONTENT

1	INTRODUCTION	3
2	STUDY AREA AND DATA SETS	3
2.1	STUDY AREA	3
2.2	AVAILABILITY OF DATA SETS	5
3	DEVELOPMENT OF A WEATHER GENERATOR FOR THE OUÉMÉ BASIN	6
3.1	INTRODUCTION	6
3.2	METHODOLOGY	7
3.2.1	Rainfall generator	7
3.2.2	Temperature generator	8
4	RESULT	9
4.1	PRECIPITATION DOWNSCALING MODEL	9
4.1.1	Calibration and validation using observations	9
4.1.2	Climate scenarios	10
4.2	TEMPERATURE DOWNSCALING MODEL	14
4.2.1	Calibration and validation using observations	14
4.2.2	Climate scenarios	15
5	CONCLUSION	18
	APPENDIX I:	19
	APPENDIX II:	23

1 Introduction

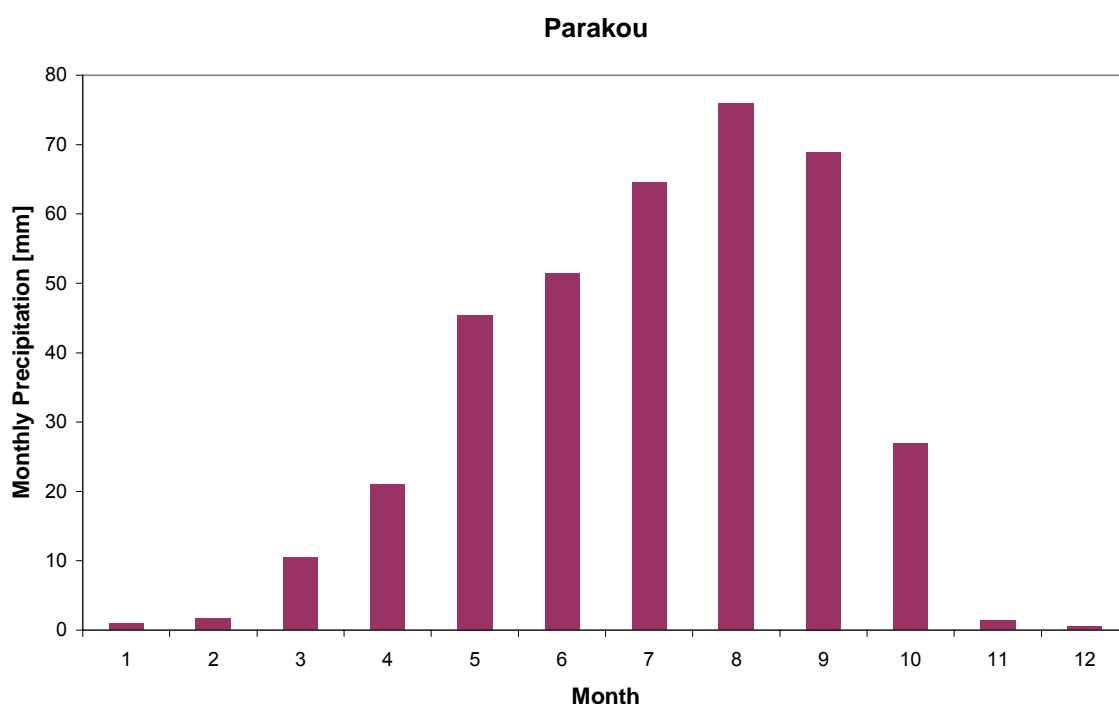
The aim of this paper is to introduce a new weather generator (WG) developed for the purpose of downscaling meteorological variables, such as precipitation and temperature for the Ouémé river basin in Benin, West Africa. The developed WG is capable of generating local variables from the output of global circulation models and fulfil the requirements of high resolution at both temporal and spatial scales. The result of this work is to be used as an input to the HBV, Epic/Slysis and Qual2K models for the integration study, in the framework of the RIVERTWIN project.

2 Study area and Data sets

2.1 Study area

The river Ouémé is the largest one within the Republic of Benin in West Africa, providing a water source for agriculture and domestic purposes. The upper Ouémé covers an area near to the southern Sahel and the lower Ouémé near to the Gulf of Guinea. The whole basin is approximately 45,000 km² and extends out over almost the entire country.

The climate there is of a typical monsoon type, which is characterized by its distinct dry and rainy seasons. Normally, the rainy seasons start from April and finish by the end of October and contribute the majority of the annual rainfall amount. However, due to the particular geophysical locations, the temporal distributions of rainfall over a year are completely different from station to station. In figure 1, three representative stations are chosen to reflect annual rainfall in the Upper, Middle and Lower catchments respectively.



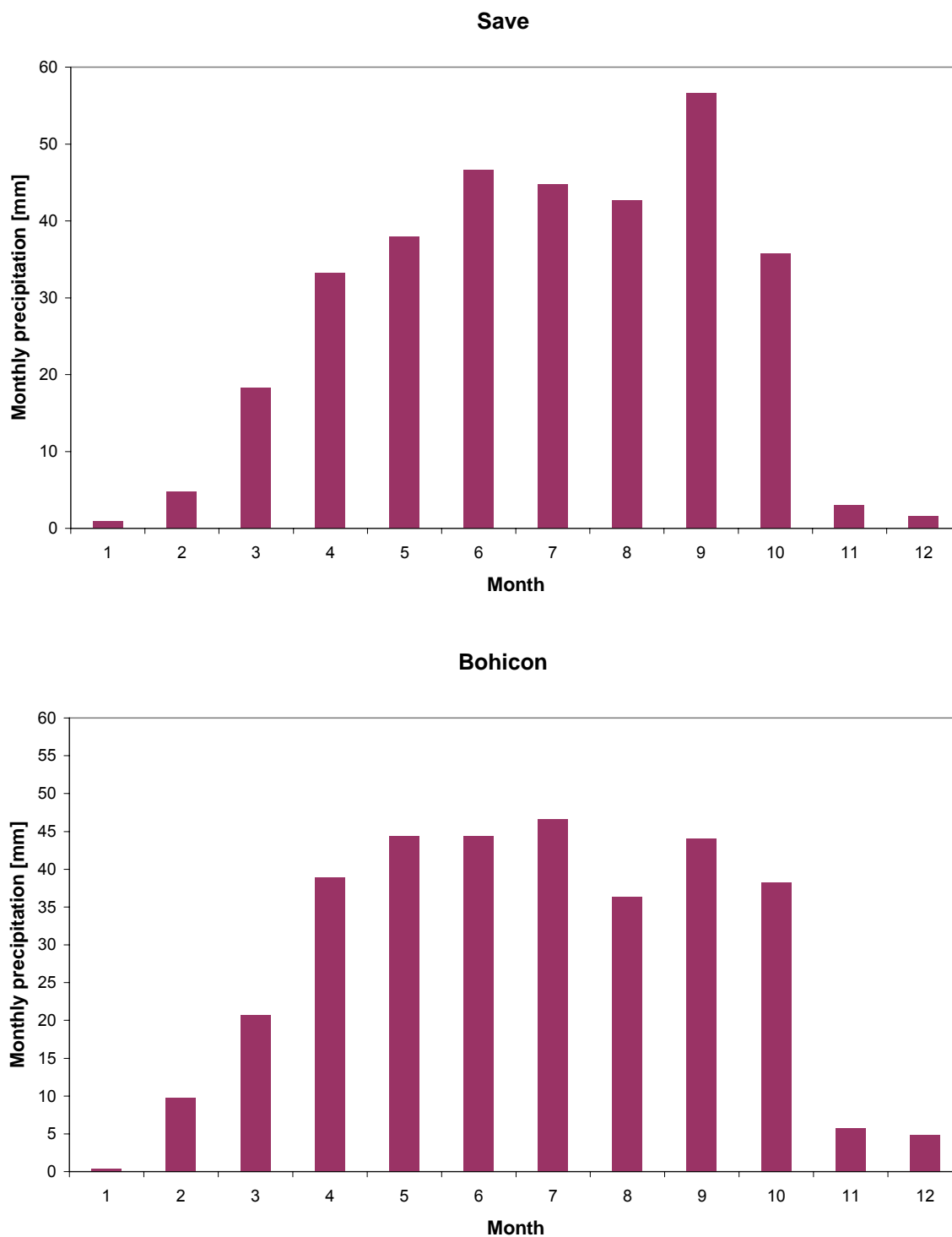


Figure 1: Representative temporal distribution of annual rainfall in the Ouémé basin

In the Upper Ouémé, near to the southern Sahel, there is only one peak that occurs from June to September; in the Middle Ouémé, the monthly precipitation of the rainy season is distributed quite evenly and there is no particular month with large rainfalls; in the Lower Ouémé, two peaks can be observed, one is normally in the middle of the big rainy season and the other is in the middle of the small rainy season.

The average temperature there is quite high, between 24° and 31°C. The difference between the annual maximum and minimum daily maximum temperature is only around 5

°C. There is no big variation amongst the dry and rainy seasons. However, the highest temperature normally occurs in dry season. The temperature in the rainy season is relatively lower.

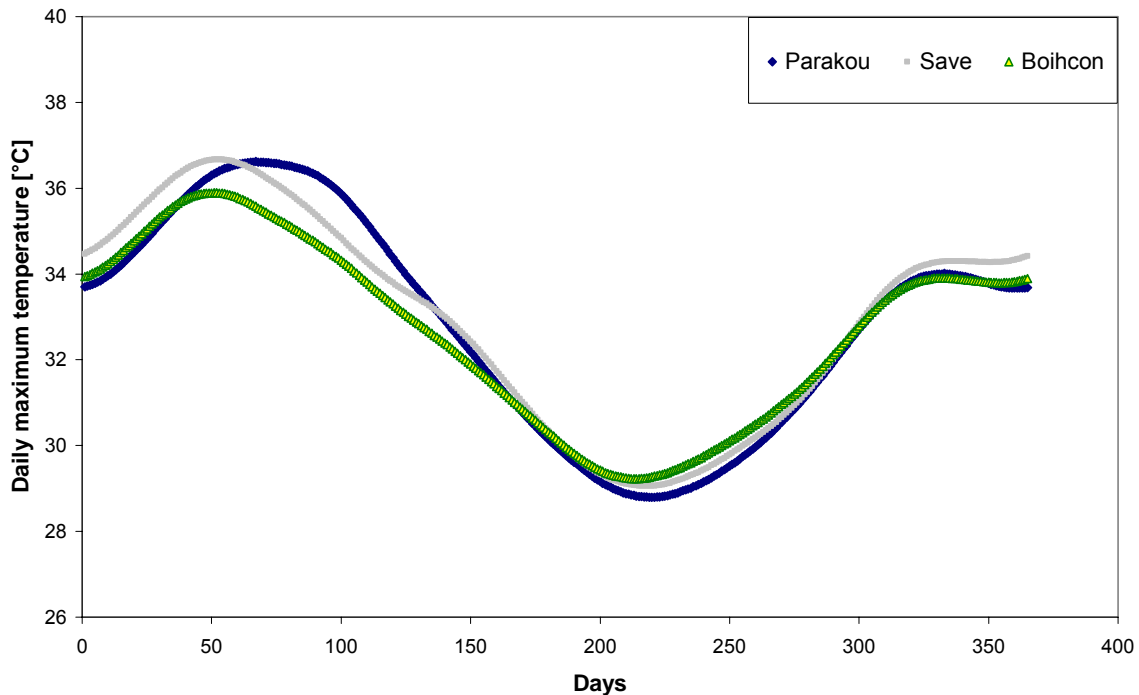


Figure 2: Annual cycle of daily maximum temperature in the Ouémé basin

2.2 Availability of data sets

Based on observation data provided by local partners, there are 133 rainfall stations and 122 temperature stations distributed over the whole river basin. However, only a few of these have been properly measured over the past 20 years. In order to fulfill the requirement of applying statistic analysis, seven rainfall stations and eight temperature stations are selected covering a time period from the year 1980 to 2003.

The time slice from the year 1980 to the year 1995 is used as calibration period and the years from 1996 to 2003 for validation.

In addition, the meteorological variables generated on a monthly basis by the global circulation model in both its control run and scenarios are adopted in order to reflect the tendency of climate changes in the next 30 years in the West Africa region and to help us further develop climate scenarios for the Ouémé river basin.

3 Development of a weather generator for Ouémé basin

3.1 Introduction

According to the basis of atmospheric science, planetary rotation causes the formation of three circulation cells in each hemisphere. Under the impact of the Coriolis force, surface air does not move directly from the equator to the poles, but deflects to the right in the northern hemisphere and to the left in the southern hemisphere.

The higher the latitude, the stronger the Coriolis force. Therefore, in the region of 30°N - 60°N in the northern hemisphere, the impact of the Coriolis force is strong. The air is swirled and finally forms distinct high and low pressure zones that provide the possibility to apply circulation pattern based downscale procedure. However, in those regions near to the equator, like the study area, the Coriolis force is close to zero. The distinguished high and low pressure system does not exist any more. A new model must be developed to reproduce an acceptable model output for the meteorological variables.

Long-term time series of meteorological variables are so frequently required for water-related models, while in reality, the observations are always inadequate. As an alternative, weather generators have been widely applied to generate synthetic time series of weather data. Presently, there are mainly two types of weather generator; one is named the Richardson's weather generator; the other is called LARs-WG.

For the Richardson's weather generator, precipitation is considered as the primary variable. Whether the day is wet or dry is applied as a condition for further generation of temperature-related variables. Therefore, the rainfall probability of a given day and amount of rain on a rainy day are required to be well formulated. Normally, the first-order Markov chain is provided to simulate the occurrence of precipitation. Either an exponential distribution or a gamma distribution is then adopted to represent a precipitation amount, given that a wet day occurs. Unlike precipitation, the temperature variables are easier to model. They are evaluated with the ARMA method, taking autocorrelation into account.

Similar to the above mentioned weather generator, the Lars-WG is also a stochastic model. However, the precipitation occurrence is simulated based on the distribution of the length of continuous sequences of dry and wet days, namely the semi-empirical distribution. The precipitation amount is generated using a mixed exponential distribution.

Unfortunately, both types of weather generator are quite site-specific, that is, they generate weather time series for a single site. To consider spatial distribution, a new weather generator needs to be developed so that weather time series at several locations can be generated simultaneously. The new model must be able to simulate the main properties of observed meteorological records, e.g., means, standard deviation, probability, and then to reproduce infinite synthetic weather time series.

3.2 Methodology

3.2.1 Rainfall generator

The **rainfall** generating model is a stochastic model that aims to reproduce key characteristics of local rainfall events. These characteristics include rainfall probability, daily mean and standard deviation of precipitation amount.

Due to its simplicity, the normal distribution is one of the widely used functions. Theoretically, it is also one of the special cases of the gamma distribution when α approaches a very large value.

$$f(x) = \frac{1}{\sigma \sqrt{2\pi}} \exp\left[-\frac{(x-\mu)^2}{2\sigma^2}\right] \quad \sigma > 0 \quad \text{Equation 1}$$

The normal distribution, generally called as gaussian distribution, has many advantages over other distributions. When the joint distribution is normally distributed, both the conditional distribution and marginal distributions of the univariate are normally distributed as well, which simplifies the problem and makes the model easier to couple with other normally distributed parameters. Therefore, many multivariate distributions are presented by normal distributions. A multivariate normal distribution can also be applied for describing precipitation. However, precipitation contains special properties. It is distinctly asymmetrical, skewed to the right and physically constrained to be non-negative. That is, small daily rainfall amounts occur quite often, while large daily rainfall, which is most important to flooding and hydraulics occurs rarely. In order to capture this specific characteristic, the power transformation is always required to correct the skewness so as to mathematically fit the Gaussian distribution. (Bárdossy and Plate, 1992).

In this paper, the skewed normal distribution is chosen for fitting rainfall time series to represent the statistic properties of precipitation.

The distribution of the daily rainfall amount at the location u is dependent on weather states, dry or wet, expressed as $Z(t, u)$.

Normal distribution:

$$Z(t, u) = \begin{cases} 0 & \text{if } W(t, u) \leq 0 \\ W(t, u)^\beta & \text{if } W(t, u) > 0 \end{cases} \quad \text{Equation 2}$$

Here,

- $Z(t, u)$: Daily precipitation amount at time t and location u
- $W(t, u)$: Normally distributed random variable for location u at time t
- β : Transformation exponent relating $Z(t, u)$ to $W(t, u)$

The parameters of the distribution are represented as μ_i and σ_i . Their annual cycle can be approximately described by the Fourier series presented by **Eq. 3 and Eq. 4**.

$$\mu_i(t^*, u) = \frac{a_0(i, u)}{2} + \sum_{k=1}^K (a_k(i, u) \cos(kwt^*) + b_k(i, u) \sin(kwt^*)) \quad \text{Equation 3}$$

$$\sigma_i(t^*, u) = \frac{c_0(i, u)}{2} + \sum_{k=1}^K (c_k(i, u) \cos(kwt^*) + d_k(i, u) \sin(kwt^*)) \quad \text{Equation 4}$$

Where t^* stands for Julian date correspondent to every actual day; $\mu_i(t^*, u)$ and $\sigma_i(t^*, u)$ are the expectation and standard deviation of precipitation on the Julian date presented by the Fourier series. a_k, b_k, c_k, d_k are the coefficients of harmonics of the Fourier series conditioned to weather states. According to the harmonic analysis, the Fourier approximation is able to be identical with the observed time series when that $t^*/2$ harmonics are introduced.

The spatial structure of rainfall is presented by a spatial covariance structure $\Gamma_{0i}(t^*)$ and $\Gamma_{li}(t^*)$, which takes spatial covariance and auto-correlation into account

The covariance structure is calculated by **Eq. 5**, where p_i and q_i are the weather state dependent and annual dependent parameters described by the Fourier series. $h(x, y)$ is the distance between pairs of stations.

$$\text{cov}[Z_x, Z_y]_{i(t)} = p_i(t^*)e^{-h(x,y)q_i(t^*)} \quad \text{Equation 5}$$

With introduction of a random number, the precipitation can be generated day by day using the following generating process:

$$W(t) = r(t^*)(W(t-1)) + C_i(t^*)\psi(t) \quad \text{Equation 6}$$

Where, t^* denotes the Julian date with respect to the consideration of annual impact. $r(t^*)$ is the autocorrelation of one-day lag to account for the previous day's impact. $\psi(t)$ is a random number $N(0, 1)$. $C_i(t^*)$ accounts for spatial variability.

3.2.2 Temperature generator

Similar to the precipitation generator, the **temperature** generator is also a stochastic model. An autoregressive moving - average method is applied to set up the model to generate daily temperature, which is a function of geopotential height on a daily basis.

The autoregressive model is built separately conditioned to the weather state, wet or dry. The time series of temperature-related variables are reduced to a sequence of residuals by moving the periodic mean and standard deviations from the original observations. These periodic means and standard deviations of variables are smoothed and illustrated using the Fourier series. In addition, the autocorrelation and cross correlation between variables are determined for the residuals that are quite time dependent and independent, respectively.

Finally, the daily maximum and minimum temperature can be generated as a simple linear regression. See **Eq. 7**.

$$x_{t+1} - \mu = \phi(x_t - \mu) + \varepsilon_{t+1} \quad \text{Equation 7}$$

4 Result

4.1 Precipitation downscaling model

4.1.1 Calibration and validation using observations

There are 7 stations out of 133 stations with a relatively long dataset in the Ouémé basin covering a time slice from 1980 to 2003. The years 1980 to 1995 were chosen to calibrate model's parameters and the remaining years were used for testifying the model's performance.

The performance of annual cycle is one of indicators to evaluate model's performance. The diagram of observed and simulated precipitation is shown in **Appendix I**. As seen from **Tab. 1**, the annual precipitation in the Ouémé river basin is averaged around 1000 mm per year, while the variability from year to year is increased from the northern to the southern stations. Our model is able to well simulate annual total precipitation for all 7 stations, but is weaker at representing inter-annual variability. The monthly totals at each station are well represented by the annual cycle in **Appendix I** and high correlation coefficient can be seen in following **Tab. 2**, though with underestimation of peak precipitation in the rainy seasons. This weakness is particularly dominant in the Southern part.

Table 1: Average and variance of annual precipitation over the years from 1980 to 1995

Station	Annual precipitation		Standard deviation	
	Observed	Simulated	Observed	Simulated
Kandi	900.8	896.3	135.9	195.4
Natitingou	1134.8	1086.7	152.2	93.4
Parakou	1148.8	1093.8	264.3	112.6
Save	1015.4	931.0	193.7	131.8
Ketou	1031.5	1055.8	201.1	126.9
Bohicon	1039.0	1021.3	211.7	169.5
Lonkly	1046.8	1020..8	307.9	156.2

Table 2: Correlation between monthly precipitations derived from observation and simulations from 1980 to 1995

Station	Correlation coefficient [r]
Kandi	0.98
Natitingou	0.98
Parakou	0.98
Save	0.96
Ketou	0.90
Bohicon	0.94
Lonkly	0.91

In order to compare the model's performance with observations, diagnostics have been applied. These diagnostic indices including average precipitation [Pav], 90th percentile of

rainy day's amounts [P90], consecutive wet days [CWD], mean wet-day persistence [Pww], mean dry-day persistence [Pdd], mean wet spell [Lw], mean dry spell [Ld] and maximum dry spell [Ldm] are recommended by the EU - funded STARDEX project. 3 stations located in the upper Ouémé, middle Ouémé and lower Ouémé respectively are selected to compare different rainfall behaviors.

Table 3: Extreme indices derived from different model's settings [Wet seasons]

Indices	Unit	Parakou (upper Ouémé)		Save (middle Ouémé)		Boihcon (Lower Ouémé)	
		Observed	Simulated	Observed	Simulated	Observed	Simulated
Pav	mm	4.91	4.86	4.41	3.87	4.26	4.04
P90	mm	34.1	36.9	32.4	31.2	35.0	34.0
CWD	day	5.3	5.1	4.95	4.6	4.75	4.42
Pww	-	0.38	0.36	0.36	0.34	0.32	0.32
Pdd	-	0.69	0.72	0.72	0.74	0.72	0.74
Lw	day	1.63	1.59	1.56	1.53	1.50	1.48
Ld	day	3.05	3.51	3.50	3.83	3.70	3.82
Ldm	day	14.7	14.67	14.55	15.08	17.5	14.38

The above table shows that the model's output generally underestimates mean precipitation over all 3 stations, while the simulated 90th percentile of precipitation is not far away from that derived from observations. The conditional probability of Pww and Pdd give out comparable results.

4.1.2 Climate scenarios

For understanding the impact of climate change on the future climate conditions in the Ouémé basin, two different scenarios, A2 and B2 generated by ECHAM4 model, are selected.

There are 3 grid-cells covering the regions inside Benin. Grid-cell 1 covers the southern part of Niger and a small part of northern Benin; grid-cell 2 covers most of the region in the Northern Benin and grid-cell 3 the region in Southern Benin. The precipitation-related and temperature-related parameters of these 3 grid-boxes derived from control run and corresponding scenarios are calculated and compared to determine the trend of climate changes in the coming 30 years. These precipitation-related parameters include the amount of monthly precipitation, the standard deviation of monthly precipitation and the probability of precipitation for each month. The temperature-related parameters consist of monthly maximum temperatures and monthly minimum temperatures.

Since the study area is in the middle and lower parts of the Ouémé basin, the behaviors of grid-cell 2 and grid-cell 3 are of interest. In the following sections, variables derived from these 2 grid-cells are used. Their corresponding results are indicated as the combination of scenario information and grid information. For instance, scenario A2-2 indicates the result derived from grid-cell 2 conditioned to A2 scenario.

The real values of those parameters are presented in **Tab. 6** to **Tab. 20** in **Appendix II**. The ratios between meteorological parameters derived from the control run and the scenarios are calculated and further applied for impact studies. See **Fig. 3** to **Fig. 5**.

As an integral response to the key properties of precipitation, the annual cycles of several stations conditioned to A2 and B2 scenarios are generated. For those stations located in the northern part, both A2 and B2 scenarios show the increase of precipitation amount in rainy seasons, especially in August. Scenario A2 even suggests more rainfall than scenario B2. For those stations located in the southern part, scenarios show out the reduction of precipitation in rainy seasons. There is no big difference between A2 and B2 scenarios. See **Fig. 6 to Fig.10**.

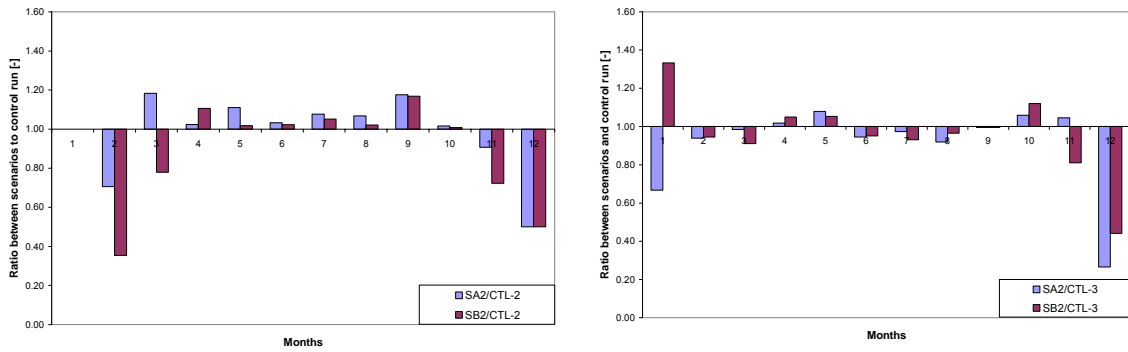


Figure 3: The ratios between monthly precipitations derived from scenarios and those from the control run [Left: Grid-cell 2; Right: Grid-cell 3]

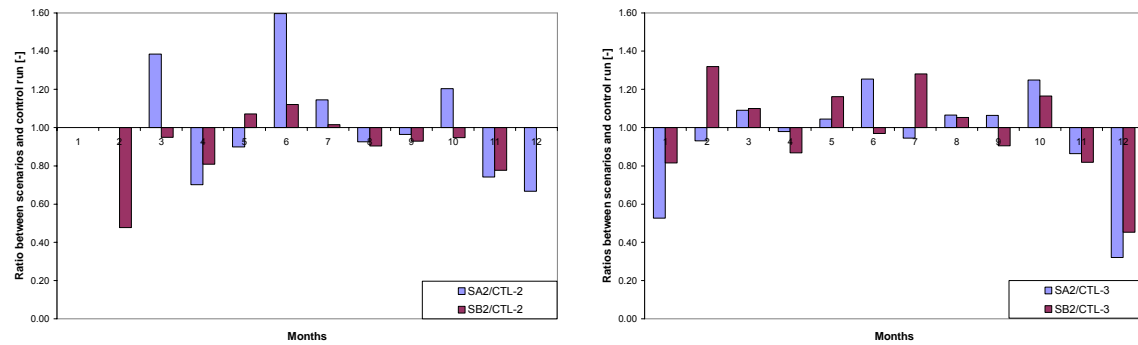


Figure 4: The ratios between standard deviation of monthly precipitations derived from scenarios and those from the control run [Left: Grid-cell 2; Right: Grid-cell 3]

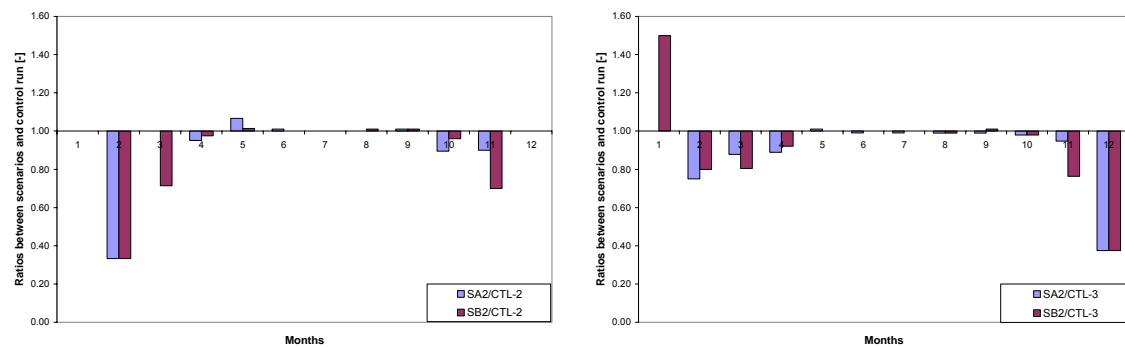


Figure 5: The ratios between probabilities of rainfall derived from scenarios and those from the control run [Left: Grid-cell 2; Right: Grid-cell 3]

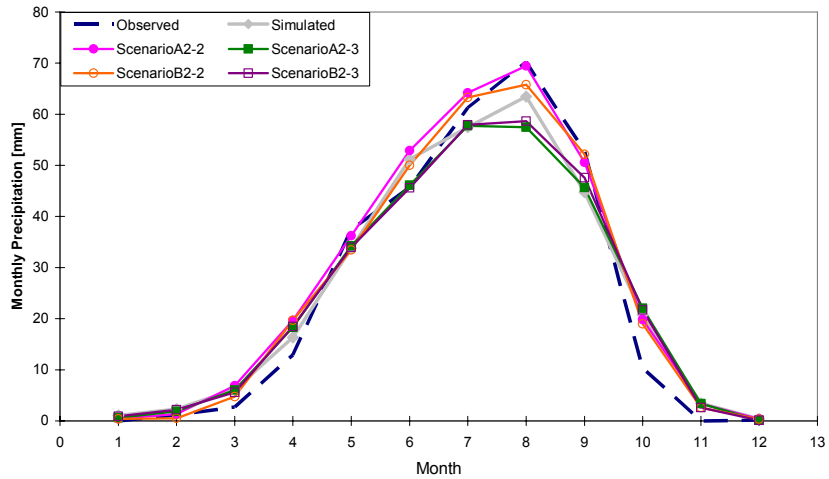


Figure 6: The comparison between monthly precipitation derived from observation, simulation and scenarios at station Kandi

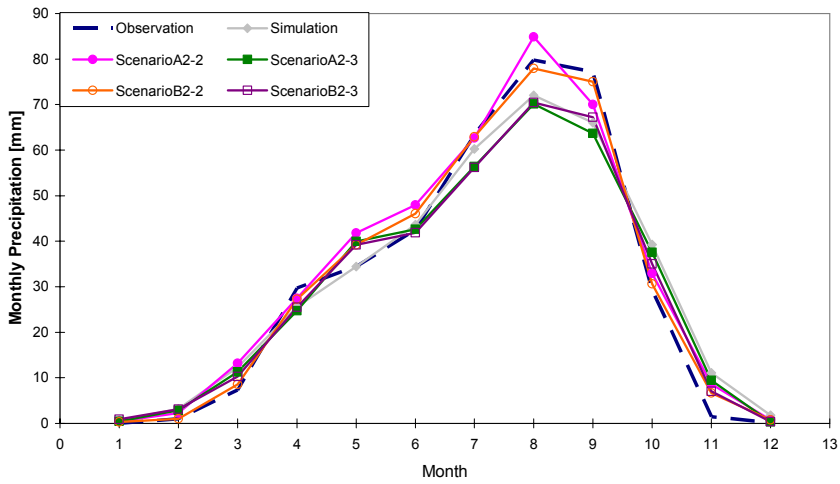


Figure 7: The comparison between monthly precipitation derived from observation, simulation and scenarios at station Natitingou

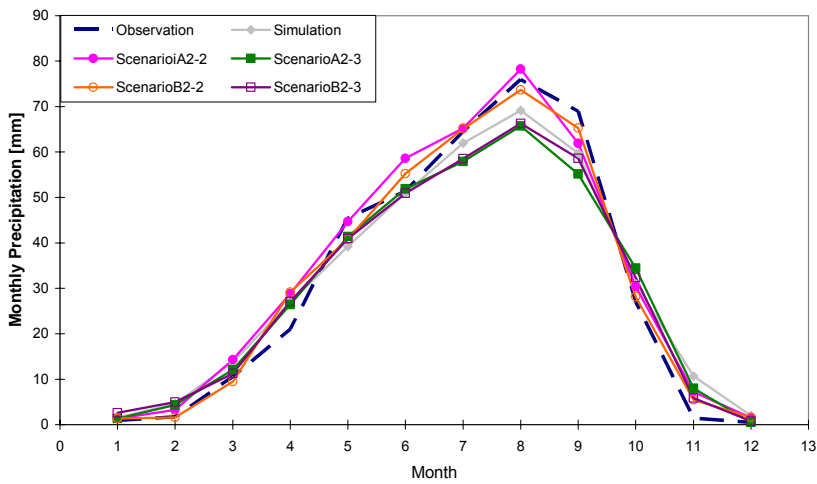


Figure 8: The comparison between monthly precipitation derived from observation, simulation and scenarios at station Parakou

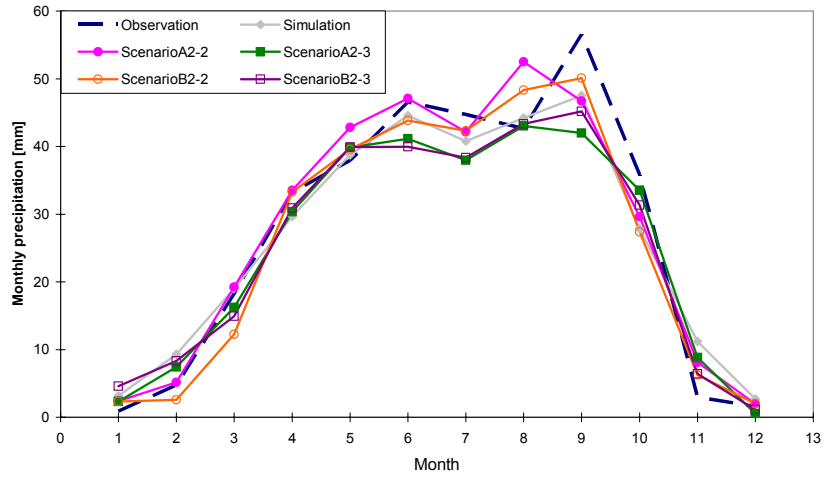


Figure 9: The comparison between monthly precipitation derived from observation, simulation and scenarios at station Save

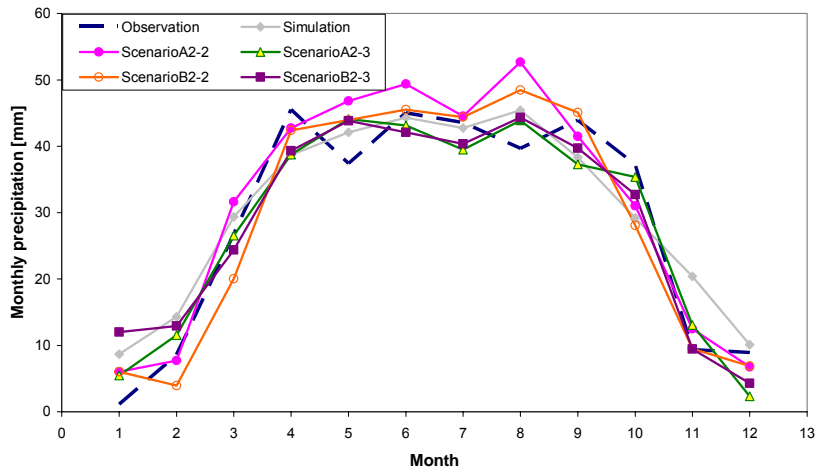


Figure 10: The comparison between monthly precipitation derived from observation, simulation and scenarios at station Lonkly

4.2 Temperature downscaling model

4.2.1 Calibration and validation using observations

8 stations out of 122 stations covering time slice from 1980 to 2003 are chosen for model's setup. The year 1980 to 1995 were chosen to calibrate model's parameters and the rest of years for model's validation.

The annual cycles of daily minimum and maximum temperature are generated for each station to compare the model's output with observations. **Fig. 11** and **Fig. 12** provide a good overview of seasonal change of daily temperature observed and simulated for stations located in the Northern and Southern parts of river basin. Stations Kandi and Parakou are located in the upper basin, station Save in the middle and station Cotonou in the lower basin near to Golf of Guinea.

Moving from the North to the South, the variation of temperature tends to be smoother and smoother. The southern region is cooler than the northern due to impact of the Gulf of Guinea. However, the peak temperature is generally in the dry season and lowest temperature in the rainy season.

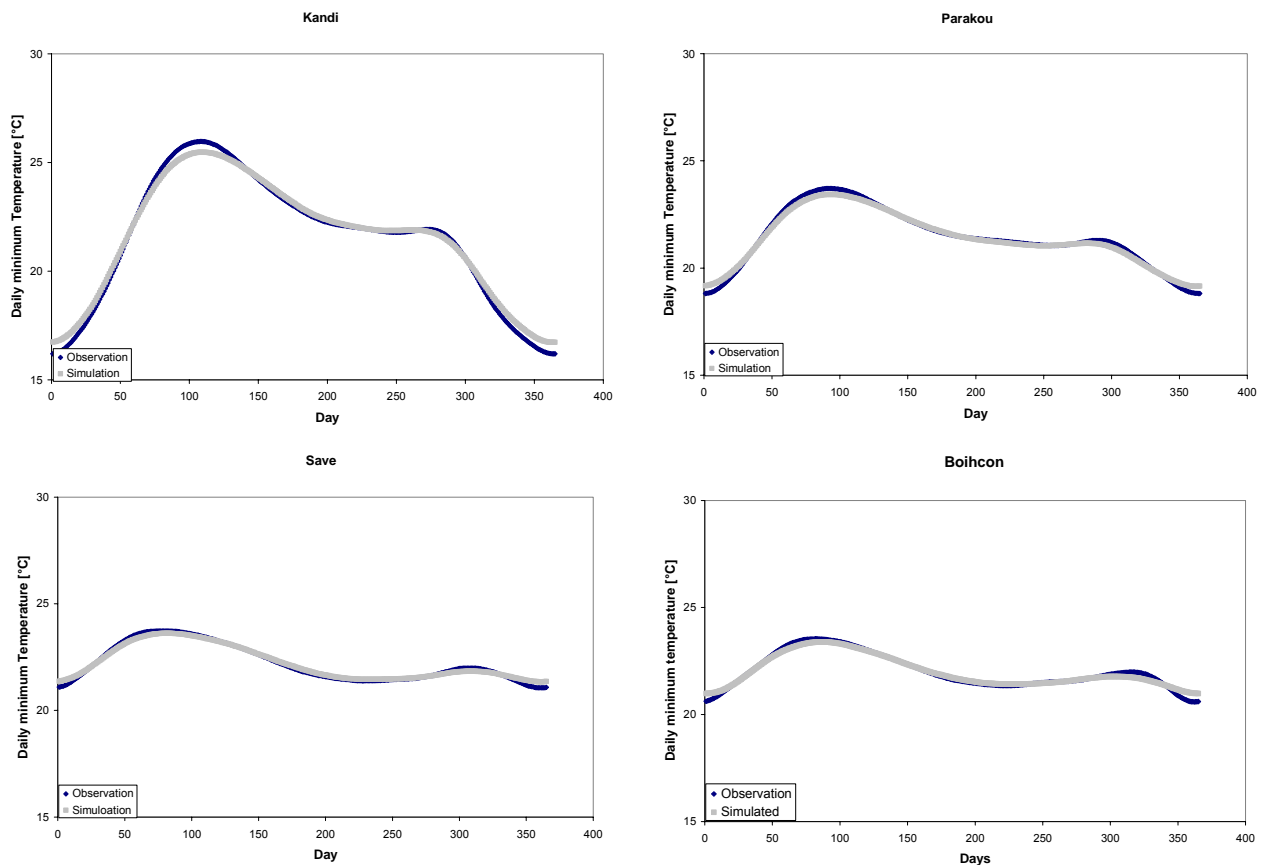


Figure 11: Daily minimum temperature derived from observation and simulations

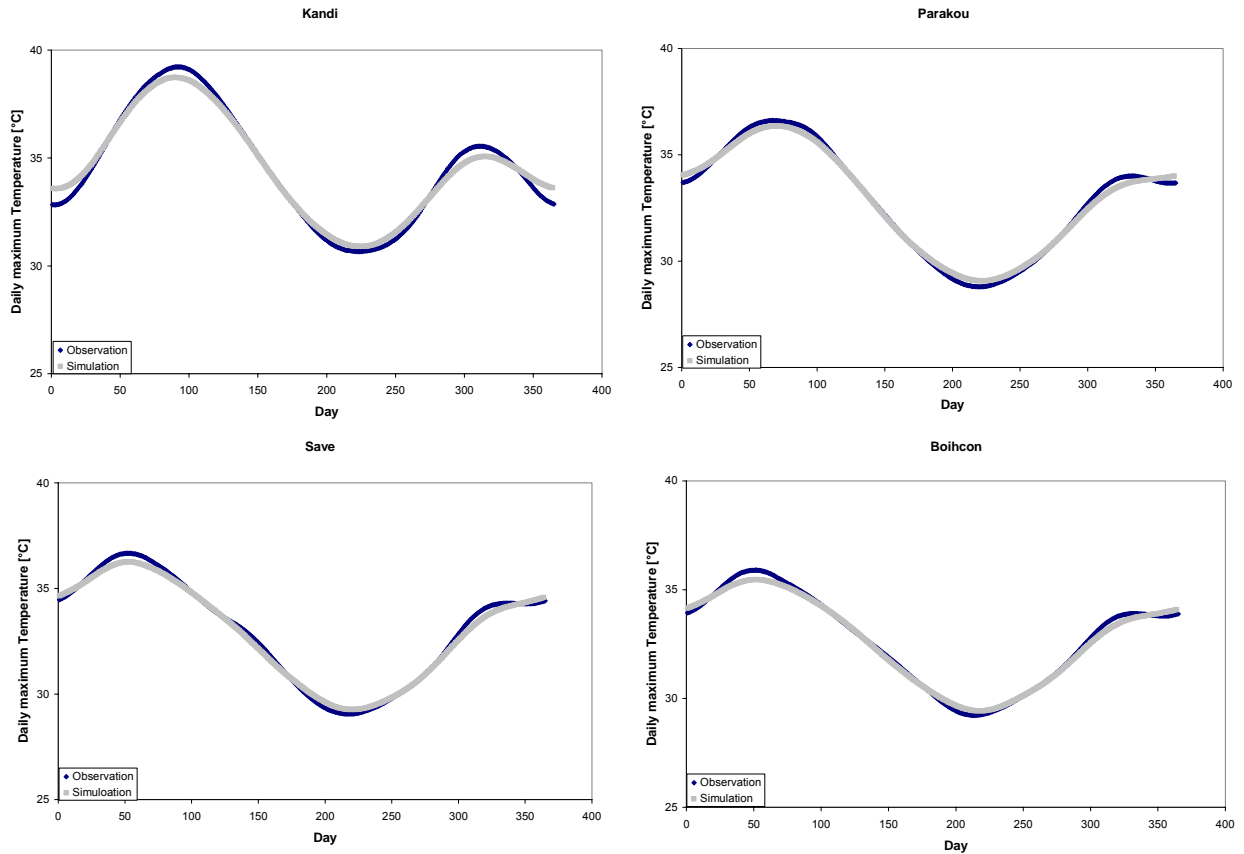


Figure12: Daily maximum temperature derived from observation and simulations

Extreme conditions are also of interest. Therefore, diagnostic analysis of those over observation and simulation are undertaken. Indices include average Tmin 10th percentile [Tmin10] and Tmax 90th percentile [Tmax90].

Table 4: Extreme indices derived from different model settings [Dry seasons]

Indices	Unit	Parakou (upper Ouémé)		Save (middle Ouémé)		Boihcon (Lower Ouémé)	
		Observed	Simulated	Observed	Simulated	Observed	Simulated
Tmin10	°C	17.4	18.2	19.6	20.4	21.2	21.8
Tmax90	°C	37.5	37.3	37.5	37.3	36.9	36.5

Table 5: Extreme indices derived from different model settings [Wet seasons]

Indices	Unit	Parakou (upper Ouémé)		Save (middle Ouémé)		Boihcon (Lower Ouémé)	
		Observed	Simulated	Observed	Simulated	Observed	Simulated
Tmin10	°C	20.0	20.0	20.5	20.5	21.2	21.3
Tmax90	°C	35.4	35.2	34.7	34.7	34.2	34.2

The above table shows that the model's outputs reach quite good agreement with observations. Therefore, the developed temperature generator can be further applied for climate change analysis for the next 30 years.

4.2.2 Climate scenarios

Prior to generating daily temperature time series, the deviation of monthly maximum temperature and minimum temperature derived from the GCM under the conditions of A2 and B2 scenarios, and a control run have been studied. The differences between scenarios and a control run at large scale were first calculated. The results are presented in the

following figures. The positive difference indicates the increase in the monthly temperature in the coming future, while the negative difference indicates the decrease in the monthly temperature in the same time period. As seen from **Fig. 13** and **Fig. 14** below, the trends are similar between A2 and B2 scenarios. In the near future, it is likely that the minimum temperature in dry seasons will increase more than in wet seasons. Contrary to that, the maximum temperature will decreased a lot in dry seasons compared with wet season.

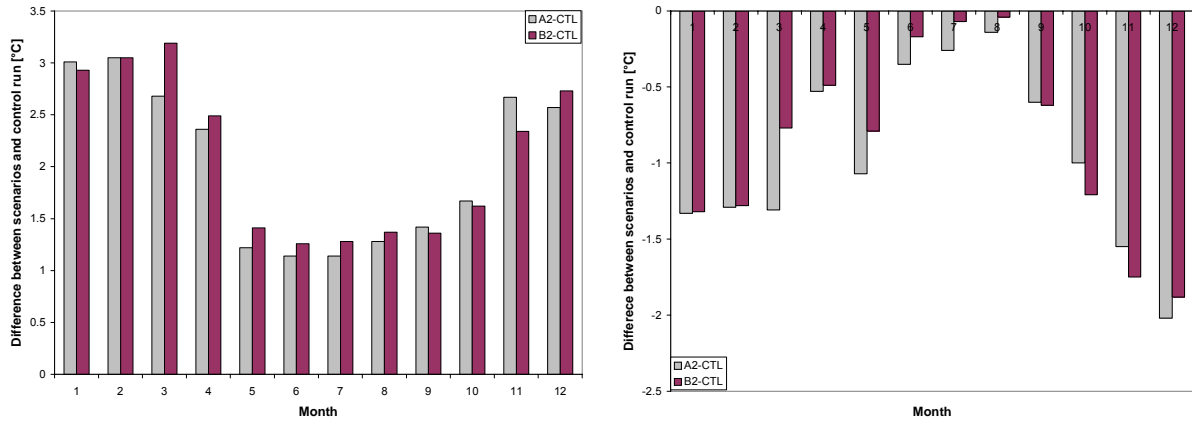


Figure 13: Difference in monthly minimum and maximum temperature derived from scenarios and control runs at grid 2 [Left: monthly minimum temperature; right: monthly maximum temperature]

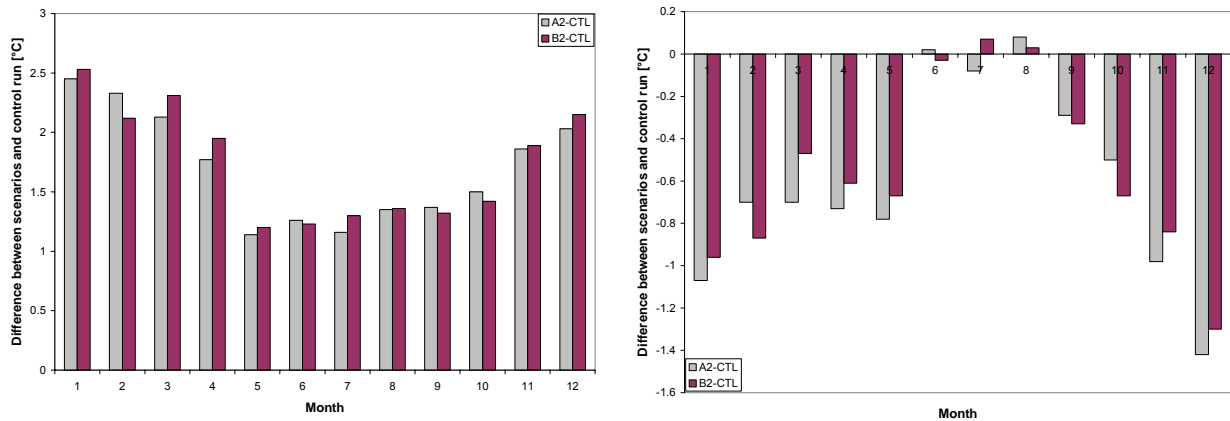


Figure 14: Difference in monthly minimum and maximum temperature derived from scenarios and control runs at grid 3 [Left: monthly minimum temperature; right: monthly maximum temperature]

As a response to climate change, the local temperature behaves as follows:

- The monthly mean maximum temperature tends to remain stable during the rainy season, but reduces by 0.8 to 2 °C during dry season.
 - There is a large increase in the monthly mean minimum temperature over the whole year; a greater increase in the dry season is expected.
 - The difference between monthly mean maximum and minimum is going to be smaller
- Conditioned to the stations located in the Ouémé basin, it can be seen that there is large variation in temperature during the dry period, with slight difference in the wet period. The daily maximum temperature tends to decrease by 1 to 2 degrees in wet and dry period

respectively, while the daily minimum temperature is likely to increase by 1.5 to 3 degrees. As a result, the daily temperature difference at each station is smaller. See **Fig. 15** and **16**.

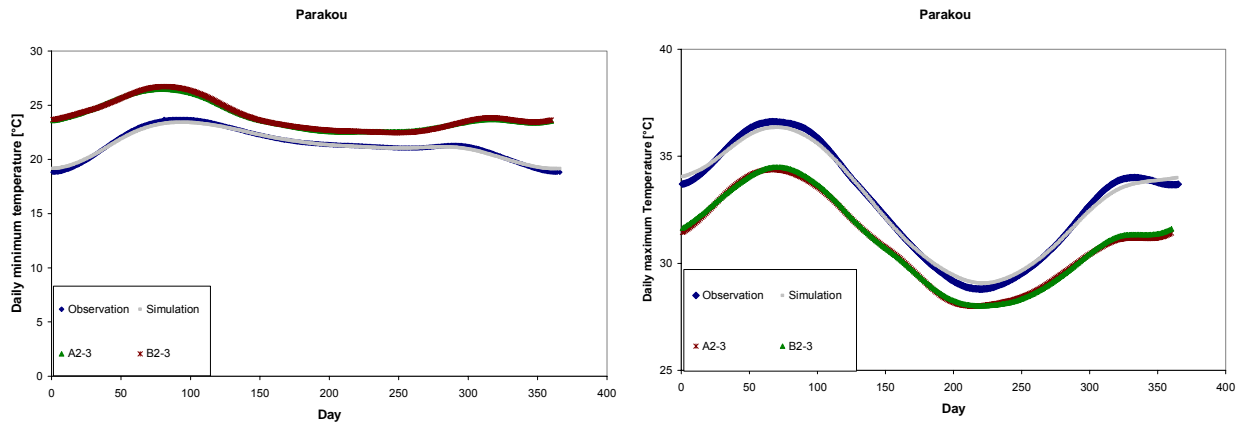


Figure 15: The annual cycle of daily minimum and maximum temperature derived from observations, simulation and scenario A2 and B2 at station Parakou [left: daily minimum temperature; right: daily maximum temperature]

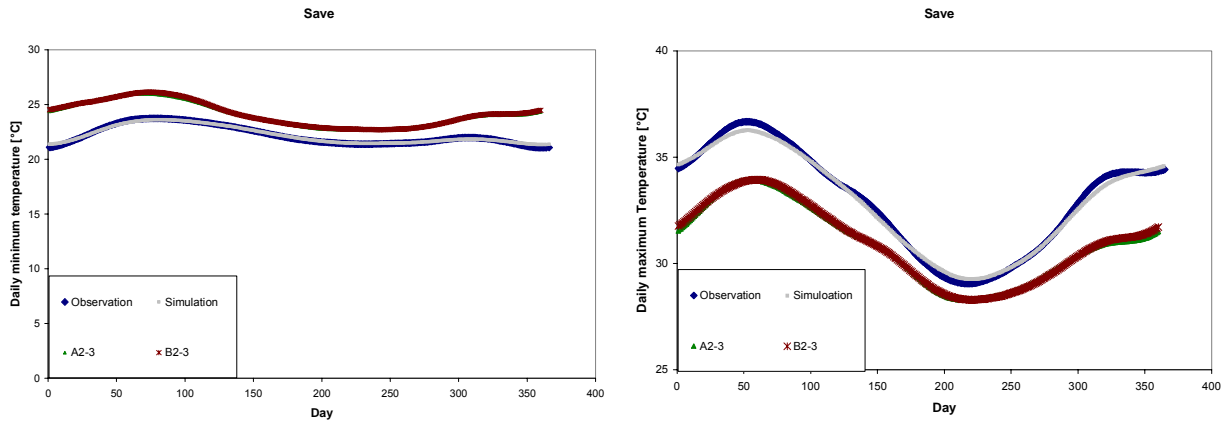


Figure 16: The annual cycle of daily minimum and maximum temperature derived from observations, simulation and scenario A2 and B2 at station Save [left: daily minimum temperature; right: daily maximum temperature]

5 Conclusion

Conditioned to the climate situation in the Ouémé river basin in Benin, a new weather generator was set up to represent a monsoon type of climate with distinct dry and wet seasons. In addition, meteorological variables could be generated simultaneously for all stations.

The model was calibrated using limited data sources. Nevertheless, there are good consistencies between observed and simulated daily precipitation and temperature, which are proved by means of the annual cycle and by diagnostic indices at selected stations. The result out of the diagnostic analysis showed that our model is able to provide a comparably good result for most features for the long term is however weaker of capturing inter-annual variability.

In order to study the impact of climate change on the future climate in study area, A2 and B2 ensembles generated by ECHAM4 were chosen to apply the impact study.

The tendency of increase in the precipitation amount in rainy seasons is noticed. For the northern part, more precipitation is suggested by the A2 scenario, compared with the B2 scenario. For the southern part, scenarios show an overall reduction of precipitation in rainy seasons. However, there is no big difference between A2 and B2 scenarios.

Daily maximum temperature remains stable during the rainy season, but is reduced by 0.8 to 2 °C during the dry season. However, there is a significant increase in daily minimum temperature during the whole year, 1.5 to 3.0 °C in the dry season and about 1.2°C in the rainy seasons. That is, the difference between daily maximum and minimum temperatures is going to be smaller.

Appendix I:

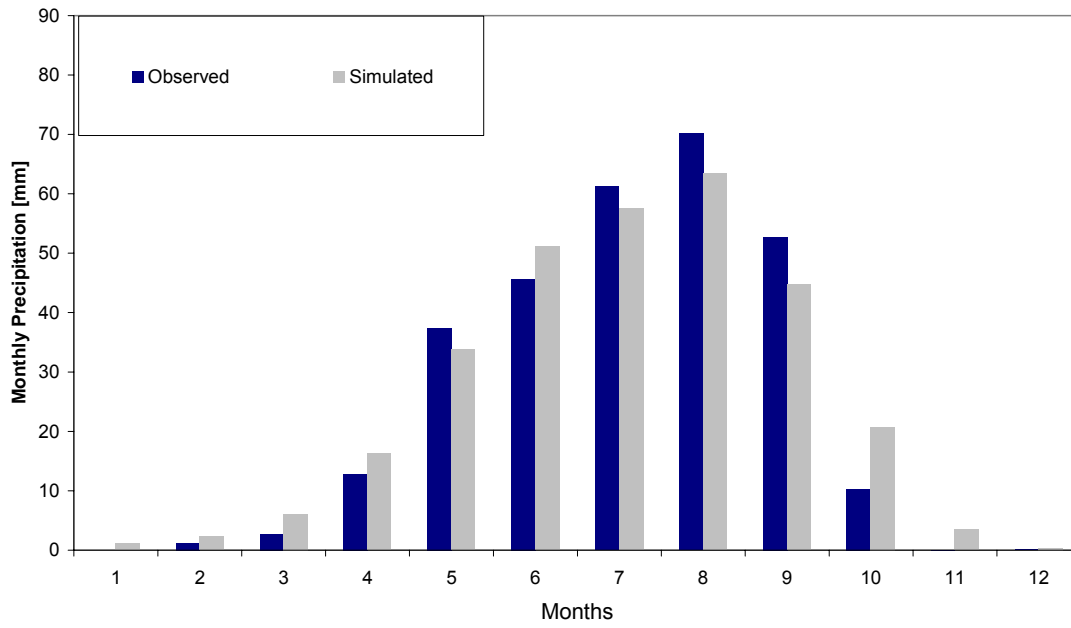


Figure 17: Annual cycle of monthly precipitation observed and simulated at station Kandi

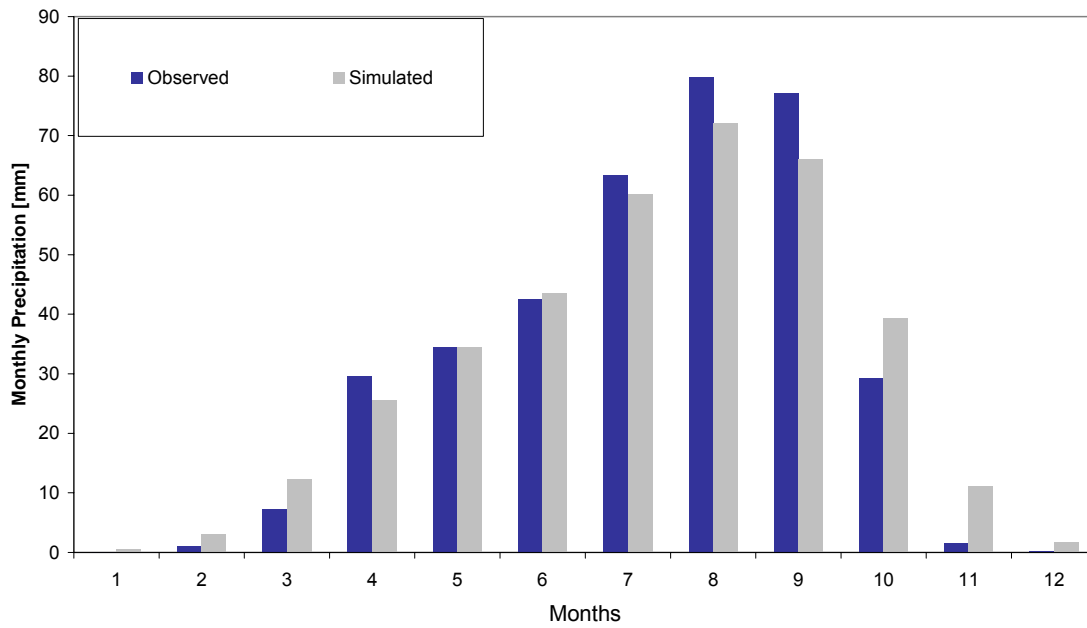


Figure 18: Annual cycle of monthly precipitation observed and simulated at station Natitingou

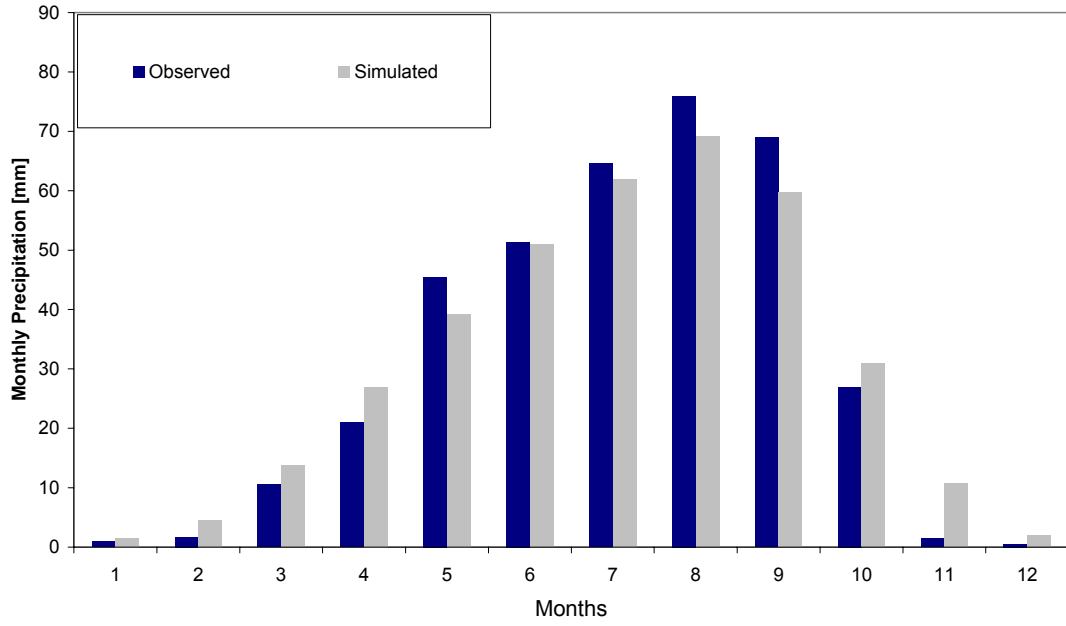


Figure 19: Annual cycle of monthly precipitation observed and simulated at station Parakou

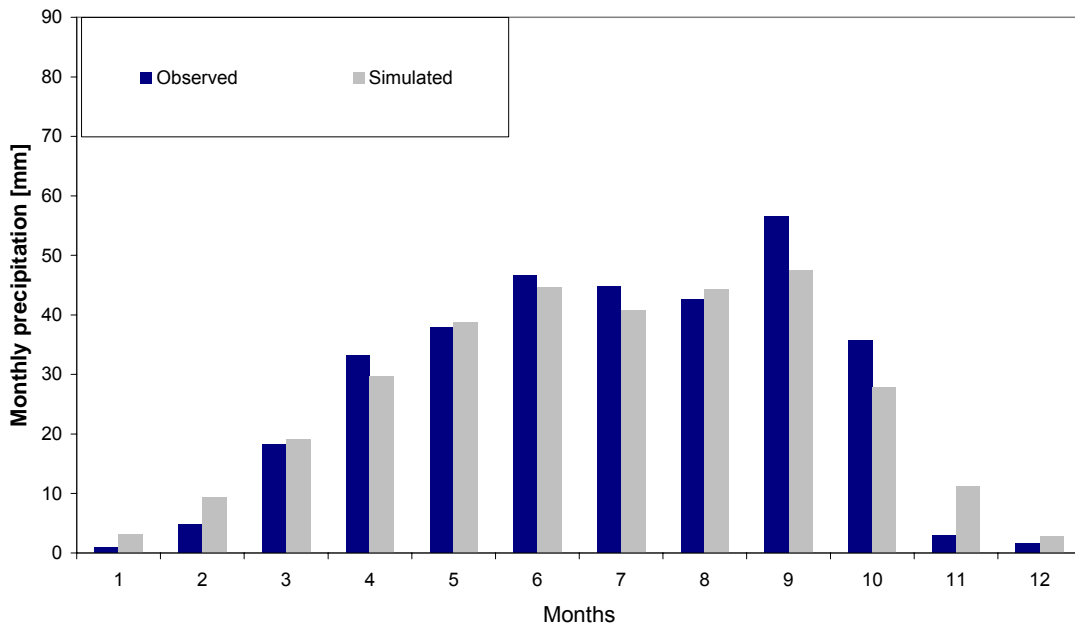


Figure 20: Annual cycle of monthly precipitation observed and simulated at station Save

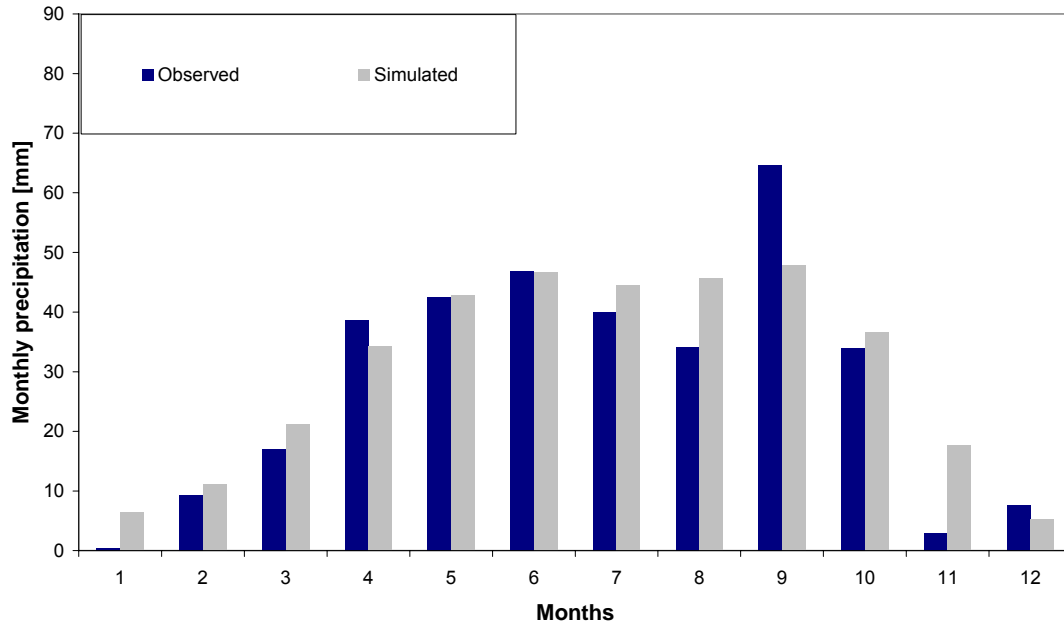


Figure 21: Annual cycle of monthly precipitation observed and simulated at station Ketou

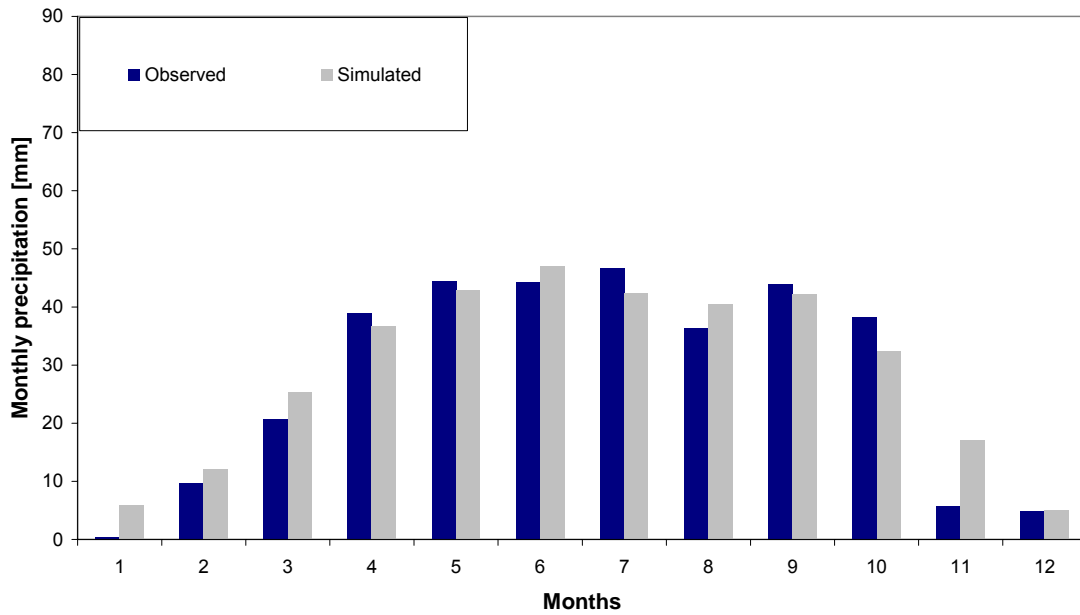


Figure 22: Annual cycle of monthly precipitation observed and simulated at station Bohicon

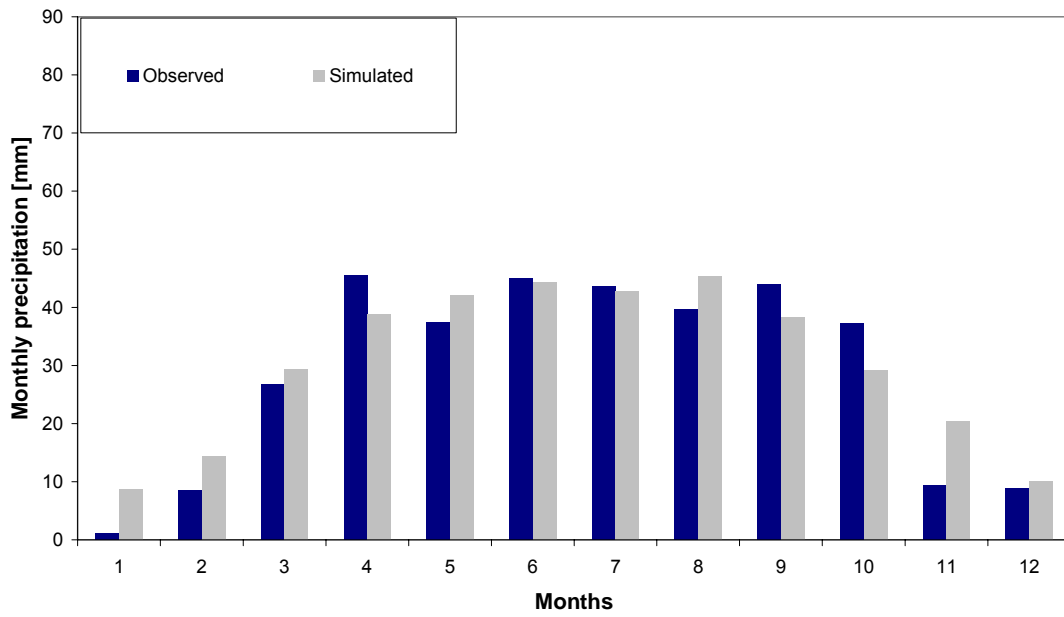


Figure 23: Annual cycle of monthly precipitation observed and simulated at station Lonkly

Appendix II:

Table 6: Daily precipitation of each month derived from control run (1960-1990)

	Jan	Feb	Mar	Apr	May	June	July	Aug	Sept	Oct	Nov	Dec
CTL-2	0.00	0.17	1.09	3.46	6.71	8.00	7.98	8.14	6.83	3.92	0.51	0.02
CTL-3	0.15	1.65	3.83	5.6	9.13	9.64	7.72	5.96	6.53	5.44	1.53	0.34

Table 7: Daily precipitation of each month derived from A2 scenarios generated by ECHAM4 (2000-2030)

	Jan	Feb	Mar	Apr	May	June	July	Aug	Sept	Oct	Nov	Dec
A2-2	0.00	0.12	1.29	3.54	7.45	8.26	8.59	8.69	8.03	3.98	0.49	0.01
A2-3	0.10	1.55	3.77	5.7	9.85	9.11	7.51	5.48	6.50	5.76	1.60	0.09

Table 8: Daily precipitation of each month derived from B2 scenarios generated by ECHAM4 (2000-2030)

	Jan	Feb	Mar	Apr	May	June	July	Aug	Sept	Oct	Nov	Dec
B2-2	0.00	0.06	0.85	3.83	6.83	8.18	8.39	8.31	7.98	3.95	0.39	0.01
B2-3	0.20	1.56	3.49	5.88	9.61	9.17	7.19	5.75	6.50	6.09	1.24	0.15

Table 9: Standard deviation of daily precipitation of each month derived from control run generated by ECHAM4 (1960-1990)

	Jan	Feb	Mar	Apr	May	June	July	Aug	Sept	Oct	Nov	Dec
CTL-2	0.00	0.44	0.99	1.57	2.08	1.66	1.31	1.36	1.41	1.33	0.85	0.06
CTL-3	0.38	1.16	1.10	1.96	2.04	2.25	1.64	1.53	1.57	1.33	1.10	0.53

Table 10: Standard deviation of daily precipitation of each month derived from A2 scenarios generated by ECHAM4 (2000-2030)

	Jan	Feb	Mar	Apr	May	June	July	Aug	Sept	Oct	Nov	Dec
A2-2	0.02	0.44	1.37	1.10	1.87	2.65	1.50	1.26	1.36	1.60	0.63	0.04
A2-3	0.20	1.08	1.20	1.92	2.13	2.82	1.55	1.63	1.67	1.66	0.95	0.17

Table 11: Standard deviation of daily precipitation of each month derived from B2 scenarios generated by ECHAM4 (2000-2030)

	Jan	Feb	Mar	Apr	May	June	July	Aug	Sept	Oct	Nov	Dec
B2-2	0.02	0.21	0.94	1.27	2.23	1.86	1.33	1.23	1.31	0.26	0.66	0.06
B2-3	0.31	1.53	1.21	1.70	2.37	2.18	2.10	1.61	1.42	1.55	0.90	0.24

Table 12: Probability of precipitation of each month derived from control run generated by ECHAM4 (1960-1990)

	Jan	Feb	Mar	Apr	May	June	July	Aug	Sept	Oct	Nov	Dec
CTL-2	0.00	0.03	0.14	0.41	0.75	0.97	0.99	0.98	0.97	0.76	0.10	0.01
CTL-3	0.02	0.20	0.41	0.63	0.93	0.99	0.99	0.98	0.98	0.95	0.38	0.08

Table 13: Probability of precipitation of each month derived from A2 scenarios generated by ECHAM4 (2000-2030)

	Jan	Feb	Mar	Apr	May	June	July	Aug	Sept	Oct	Nov	Dec
A2-2	0.00	0.01	0.14	0.39	0.80	0.98	0.99	0.98	0.98	0.68	0.09	0.01
A2-3	0.02	0.15	0.36	0.56	0.94	0.98	0.98	0.97	0.97	0.93	0.36	0.03

Table 14: Probability of precipitation of each month derived from B2 scenarios generated by ECHAM4 (2000-2030)

	Jan	Feb	Mar	Apr	May	June	July	Aug	Sept	Oct	Nov	Dec
B2-2	0.00	0.01	0.10	0.40	0.76	0.97	0.99	0.99	0.98	0.73	0.07	0.01
B2-3	0.03	0.16	0.33	0.58	0.93	0.99	0.99	0.97	0.99	0.93	0.29	0.03

Table 15: Daily maximum temperature derived from control run generated by ECHAM4 (1960-1990)

	Jan	Feb	Mar	Apr	May	June	July	Aug	Sept	Oct	Nov	Dec
CTL-2	32.3	35.5	37.7	36.1	31.5	27.3	26.5	26.6	27.9	29.9	33.2	32.1
CTL-3	33.6	35.6	35.6	33.5	29.8	27.1	26.8	26.9	27.7	28.7	31.3	32.5

Table 16: Daily maximum temperature derived from A2 scenarios generated by ECHAM4 (2000-2030)

	Jan	Feb	Mar	Apr	May	June	July	Aug	Sept	Oct	Nov	Dec
A2-2	31.0	34.2	36.4	35.6	30.5	26.9	26.2	26.4	27.3	28.9	31.6	30.1
A2-3	32.6	34.8	34.9	32.8	29.0	27.2	26.7	27.0	27.5	28.2	30.4	31.1

Table 17: Daily maximum temperature derived from B2 scenarios generated by ECHAM4 (2000-2030)

	Jan	Feb	Mar	Apr	May	June	July	Aug	Sept	Oct	Nov	Dec
B2-2	30.9	34.1	36.8	35.5	30.6	26.9	26.3	26.4	27.2	28.6	31.3	30.1
B2-3	32.5	34.5	34.9	32.8	29.0	27.0	26.7	26.8	27.3	27.9	30.4	31.1

Table 18: Daily minimum temperature derived from control run generated by ECHAM4 (1960-1990)

	Jan	Feb	Mar	Apr	May	June	July	Aug	Sept	Oct	Nov	Dec
CTL-2	23.1	25.8	28.4	29.0	26.5	24.3	23.8	23.8	24.1	24.5	24.5	22.7
CTL-3	25.4	28.1	28.9	27.7	26.0	24.6	24.2	24.2	24.6	24.7	25.4	24.8

Table 19: Daily minimum temperature derived from A2 scenarios generated by ECHAM4 (2000-2030)

	Jan	Feb	Mar	Apr	May	June	July	Aug	Sept	Oct	Nov	Dec
A2-2	26.1	28.8	31.0	31.3	27.7	25.4	24.9	25.0	25.5	26.1	27.2	25.2
A2-3	27.8	30.4	31.0	29.5	27.2	25.0	25.4	25.5	25.5	26.0	27.9	26.9

Table 20: Daily minimum temperature derived from B2 scenarios generated by ECHAM4 (2000-2030)

	Jan	Feb	Mar	Apr	May	June	July	Aug	Sept	Oct	Nov	Dec
B2-2	25.9	28.7	31.4	31.3	27.8	25.4	24.9	25.0	25.3	26.0	26.7	25.2
B2-3	27.8	30.1	31.1	29.5	27.1	25.7	25.4	25.5	25.8	26.0	27.2	26.9